

## Testing and Comparing the Inhibitory Action of Red Onion Seeds and Peels Extracts on the Corrosion of Steel in Phosphoric Acid

*Ehteram A. Noor*<sup>\*</sup>, *Aisha Al-Moubaraki*, *Aqlah H. Al-Zhrani* and *Manal H. Hubani*

King Abdulaziz University, Science Faculty, Chemistry Department, Jeddah, Saudi Arabia.

\*E-mail: [m7o7o7n@hotmail.com](mailto:m7o7o7n@hotmail.com)

*Received:* 3 March 2016 / *Accepted:* 3 June 2016 / *Published:* 7 July 2016

---

The inhibitory action of Red onion seeds and peels extracts (ROSE & ROPE) was testing and comparing on the corrosion of steel in 0.75 M H<sub>3</sub>PO<sub>4</sub> using chemical measurements (hydrogen evolution, HE and mass loss, ML) and SEM technique. The effect of temperature on the corrosion of steel in 0.75 M H<sub>3</sub>PO<sub>4</sub> without and with certain concentration of each extract was studied in the temperature range of 303–333 K. Generally, the inhibition efficiency (i.e. surface coverage) increases with extracts concentration and fits the Langmuir adsorption isotherm. The results of HE, ML and SEM showed that ROSE has a capability to protect steel surface in 0.75 M H<sub>3</sub>PO<sub>4</sub> more than ROPE. Good agreement between HE and ML measurements was obtained. Temperature coefficients without and with each extract revealed somewhat chemisorptive and physisorptive behavior of ROSE and ROPE, respectively. Good correlation between the major effective constituents of each extract and the inhibition mechanism was obtained.

---

**Keywords:** steel; corrosion inhibition; phosphoric acid; red onion; SEM

### 1. INTRODUCTION

Steel is the base metal alloy extensively used in manufacturing today around the world in nearly every industry [1]. For long-term structural applications like pipes, bridges, trains and ships, corrosion is the most important problem that should be overcome in order to use steel safely. Corrosion of steel is electrochemical in nature [2]. Four essential elements include the anode, the cathode, an electrical path and an electrolyte are necessary to operate a corrosion cell. In the light of this, aqueous acid solutions are superior environment for steel corrosion as it reacts with hydrogen ion and serves as both the anode and the cathode according to the following equation:



Hydrogen bubbles evolved at the cathode while the iron is oxidized at the anode and consequently lost its weight. The rate of anodic reaction is usually controlled by the rate of the cathodic reaction. So, high concentration of  $\text{H}^+$  ions (i.e., concentrated acid) promotes the corrosion rate, because there is a large capacity for consuming electrons [3]. Various acid solutions are used for metal surface treatment to remove impurities, such as stains, inorganic contaminants, rust or scale. The use of acid solutions to clean metal products is called pickling [4]. Generally, phosphoric acid ( $\text{H}_3\text{PO}_4$ ) is used in surface cleaning of steel such as chemical and electrolytic polishing, chemical and electrochemical etching and removal of oxide layers [5]. In view of the fact that  $\text{H}_3\text{PO}_4$  reacts with the treatable steel, acid concentrations and solution temperatures must be kept under control to assure desired pickling rates. Moreover, acid pickling inhibitors are used majorly in pickling baths to prevent metal corrosion and the subsequent hydrogen evolution [6]. In general, the use of corrosion inhibitors has become one of the foremost methods for reducing corrosion rate [7]. Nowadays, according to the literature, corrosion inhibitors can be classified into two categories: (i) synthetic inorganic and/or organic compounds and (ii) natural products such as plant extract, essential oils and isolated purified compounds. The use of natural products as corrosion inhibitors reflects well the so called green chemistry and give a wide spectrum of environmentally friendly inhibitors. Nevertheless, the inhibitor choice and design process for a particular corrosion system as a rule follows a common process of identifying the corrosion threats, assessing the possible rate and risks and the necessary inhibitor performance requirements [8]. To achieve these goals enormous number of scientific investigations had been done and listed in the literature which based on testing of various inhibitors for steel corrosion in acidic solutions. By reviewing these investigations, it was found that the corrosion inhibition of steel in  $\text{H}_3\text{PO}_4$  solutions using either organic compounds [9-19] or natural products [20-29] had been covered fairly. Regardless the type of inhibitor, most of the authors discussed the inhibition data on the bases of adsorption mechanism (physical adsorption and/or chemisorption) for the inhibitor species on the metal surface via their active centers. Thus the adsorbed film acts as a barrier between metal surface and the aggressive solution. Consequently the corrosion rate is reduced.

The present work aimed to test and compare the inhibitory action of red onion seeds extract (ROSE) and red onion peels extract (ROPE) on the corrosion of steel in 0.75 M  $\text{H}_3\text{PO}_4$  using chemical measurements (hydrogen evolution, HE, and mass loss, ML). Surface morphology of steel without and with certain concentration of each extract is studied using Scanning Electron Microscopy (SEM) technique. The effect of solution temperature on the inhibition efficiency is also evaluated. A possible inhibitive mechanism is suggested from the viewpoint of adsorption.

## 2. MATERIALS AND METHODS

### 2.1. Materials

Steel (0.280% C, 0.220% Si, 0.730% Mn, 0.015% P, 0.006% S, 0.007% N and the remainder Fe) is used. The aggressive solution (0.75 M  $\text{H}_3\text{PO}_4$ ) is prepared by dilution of AR grade (85% )  $\text{H}_3\text{PO}_4$  with deionized water. Red onion seeds, Fig. 1-a, were purchase from natural products market.

Fresh red onions were obtained from local supermarket in Jeddah city. Onions were carefully peeled and the outermost solid rings were collected (Fig. 1-b) and kept in dry place at room temperature.

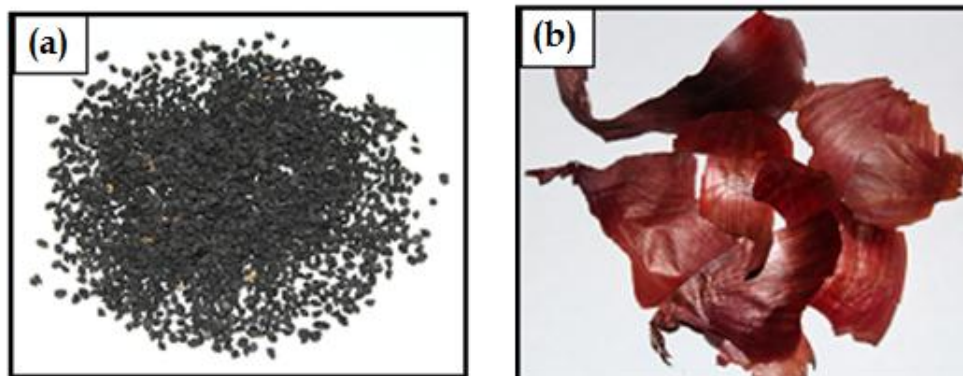


**Figure 1.** Red onion (a) seeds and (b) peels.

## 2.2. Methods

### 2.2.1. Preparation of ROSE and ROPE

The dried red onion seeds and peels were crushed and 25 g of each material individually was mixed with 250 mL of deionized water in round flask and placed on boiling water bath for 1 hour. Stirring the mixture during this interval enhances the extraction. Both extracts were left all night and then filtered and completed to 250 mL by deionized water [30]. The inhibited solutions are prepared by adding appropriate volume of the inhibitor extract to the acid solution during dilution in 100 mL measuring flask. The tested concentrations of ROSE and ROPE are in the range from 0.25 to 25 mL% (V/V%).

### 2.2.2. Preparation of steel sample

Steel samples of: (i) 1 cm in diameter and 5 cm in length (chemical study) and (ii) 1 cm in diameter and 0.5 cm in length (SEM) were cut. Before measurements, the steel samples were mechanically abraded using a series of emery papers starting with a coarse one and proceeding in steps to fine grade, rinsed with deionized water, degreased with ethanol and finally dried with a stream of air.

### 2.2.3. Chemical measurements

Figure 2 illustrates the apparatus used for chemical measurements (HE and ML). Fifty mL of 0.75 M  $\text{H}_3\text{PO}_4$  solution without or with certain concentration of inhibitor was introduced in a cell of Mylius type and a degreased, weighed steel sample was carefully dropped into the studied solution and the cell was quickly closed to ensure that no hydrogen gas escape during the experiment. The evolved  $\text{H}_2$  gas was collected by downward displacement of water and its volume was recorded at different

time intervals. A plot of evolved  $H_2$  gas per unit area ( $mL.cm^{-2}$ ) versus time (min.) gives a straight line.

The slope of the straight line represents the rate of  $H_2$  evolution ( $\rho_{HE} = dV/dt$ ) [31]. At the end time of each experiment, the steel sample was separated from the tested solution, washed thoroughly with deionized water followed by ethanol and dried with a stream of air, then weighed again. Using the difference between the mass of the studied sample before and after immersion ( $\Delta m$ ) as well as the end time ( $t_\infty$ ), the rate of mass loss ( $\rho_{ML}$ ) can be calculated as follows [31]:

$$\rho_{ML} = \frac{\Delta m}{S t_\infty} \quad (2)$$

where  $S$  is the surface area of steel sample. All experiments were conducted in stagnant solutions at 298 K except otherwise stated.

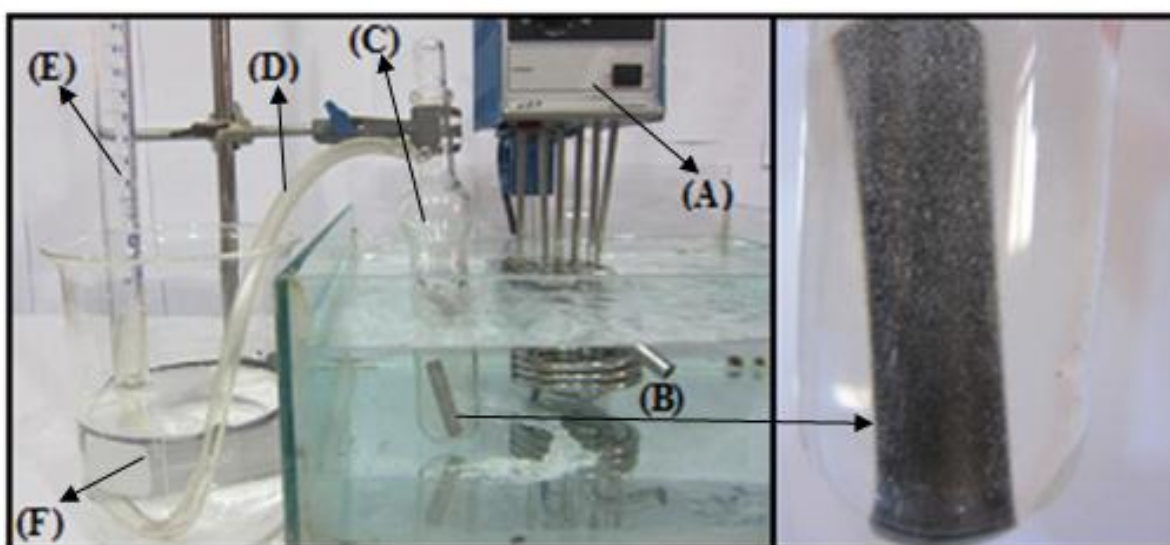


**Figure 2.** The system used for chemical measurements: (A) Thermostat ( $\pm 0.1^\circ C$ ), (B) Steel sample, (C) Mylius cell, (D) Polyethylene tube, (E) Calibrated burette filled with water and (F) Beaker (1L) half filled with water.

#### 2.2.4. SEM

An electron microscope Quanta FEG 450 was used to examine the surface morphology of steel after immersion for 90 min. in 0.75 M  $H_3PO_4$  solution without and with certain concentration of ROSE and ROPE at 298 K. The samples were rinsed gently with deionized water, degreased with ethanol, then dried carefully with a stream of air and subjected to scanning electron microscopic examination with no further treatment.

### 3. RESULTS AND DISCUSSION

#### 3.1. Effect of ROSE and ROPE concentration

The variation of the evolved hydrogen gas as a function of contact time when steel samples were immersed in 0.75 M H<sub>3</sub>PO<sub>4</sub> solution without and with various concentration of each extract was illustrated in Fig. 3.

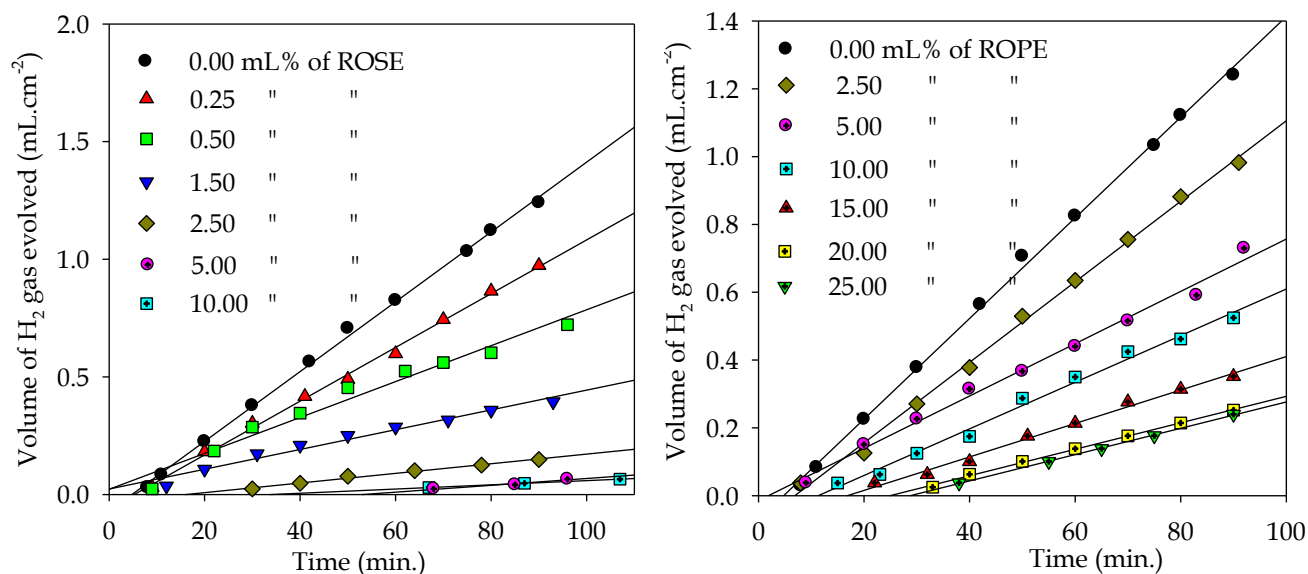


**Figure 3.** Variation of hydrogen evolved as a function of time for steel in 0.75 M H<sub>3</sub>PO<sub>4</sub> without and with different concentrations of ROSE and ROPE.

**Table 1.** Steel corrosion rates in 0.75 M H<sub>3</sub>PO<sub>4</sub> without and with different concentrations of ROSE and ROPE

$C_{extract}$ (mL%)	ROSE		$C_{extract}$ (mL%)	ROPE	
	$\rho_{HE} \times 10^3$ (mL.cm <sup>-2</sup> .min <sup>-2</sup> )	$\rho_{ML} \times 10^5$ (g. cm <sup>-2</sup> .min <sup>-2</sup> )		$\rho_{HE} \times 10^3$ (mL.cm <sup>-2</sup> .min <sup>-2</sup> )	$\rho_{ML} \times 10^5$ (g. cm <sup>-2</sup> .min <sup>-2</sup> )
0.00	14.85	3.40	0.00	14.85	3.40
0.25	11.42	2.46	2.50	11.88	2.52
0.50	7.63	1.84	5.00	7.71	1.82
1.50	4.20	1.16	10.00	6.87	1.49
2.50	2.05	0.63	15.00	4.93	1.33
5.00	1.45	0.45	20.00	3.90	1.01
10.00	0.89	0.37	25.00	3.87	0.86

It is clear that the addition of both extracts inhibits hydrogen evolution as all related solutions give lines placed under the blank solution and befall far away with increasing extract concentration.

Inspection of Fig. 3 shows the existence of incubation period ( may be due to oxide film formed naturally on the steel surface) follows by an increase in the volume of hydrogen evolved with time linearly [32]. This period was found to increase with increasing the concentration of both extracts (more pronounced in the case of ROSE), indicating the inhibitory action of both extracts against steel corrosion in 0.75 M H<sub>3</sub>PO<sub>4</sub> solution and its dependence on the extract concentration.

Table 1 gives the estimated values of steel corrosion rate in 0.75 M H<sub>3</sub>PO<sub>4</sub> solutions without and with various concentrations of ROSE and ROPE using HE and ML measurements. The values of inhibition efficiency percentage (*IE%*) at various inhibitor concentrations were calculated by the general equation:

$$IE\% = \left( \frac{\rho^o - \rho_{inh}}{\rho^o} \right) \times 100 \tag{3}$$

where  $\rho^o$  and  $\rho$  are the corrosion rates without and with certain concentration of inhibitor. The effect of ROSE and ROPE on *IE%* is graphically represented in Figure 4.

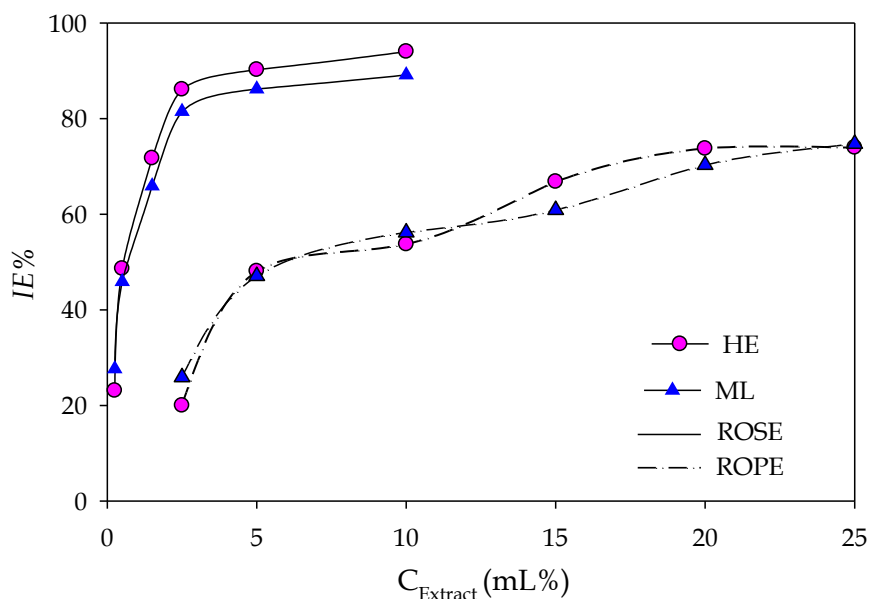


**Figure 4.** Variation of *IE%* as a function of extract concentration for steel in 0.75 M H<sub>3</sub>PO<sub>4</sub> with different concentrations of ROSE and ROPE.

Results obtained from Table 1 and Fig. 4 revealed good agreement between HE and ML measurements and as the concentration of each extract increases, the corrosion rate ( $\rho_{HE}$ ,  $\rho_{ML}$ ) decreases and the corresponding value of *IE%* increases. The overall results indicate that under identical concentrations of both extracts (2.50%, 5.00%, and 10.00 mL%), as compared to ROPE, ROSE shows superior performance as corrosion inhibitor. More confirmation for this result can be obtained by examining steel surface after immersion in 0.75 M H<sub>3</sub>PO<sub>4</sub> solution without and with identical concentration (5.00 mL%) of ROSE and ROPE for 90 min. using SEM of the same magnification, see Fig. 5. Figure 5-a shows that steel surface exposed to the aggressive solution

without inhibitor was severely attacked as indicated by the accumulation of irregular, thick corrosion products on the surface.

Figure 5-b shows dramatically decrease in the solution corrosivity with the addition of 5.00 mL% of ROSE ( $IE\% = 86.18$ ). In this case the surface is nearly undamaged as even the scratches of surface pretreatment can be observed. On the other hand, with the addition of 5.00 mL% of ROPE the corrosion rate decreases somewhat ( $IE\% = 47.06$ ) and the corrosion products layer seems smoother than that without inhibitor, see Fig. 5-c. The observed features of steel surface after immersion in 0.75 M  $H_3PO_4$  solution with ROSE and ROPE (5.00 mL%) indicates that ROSE has higher capability to protect steel surface than ROPE.

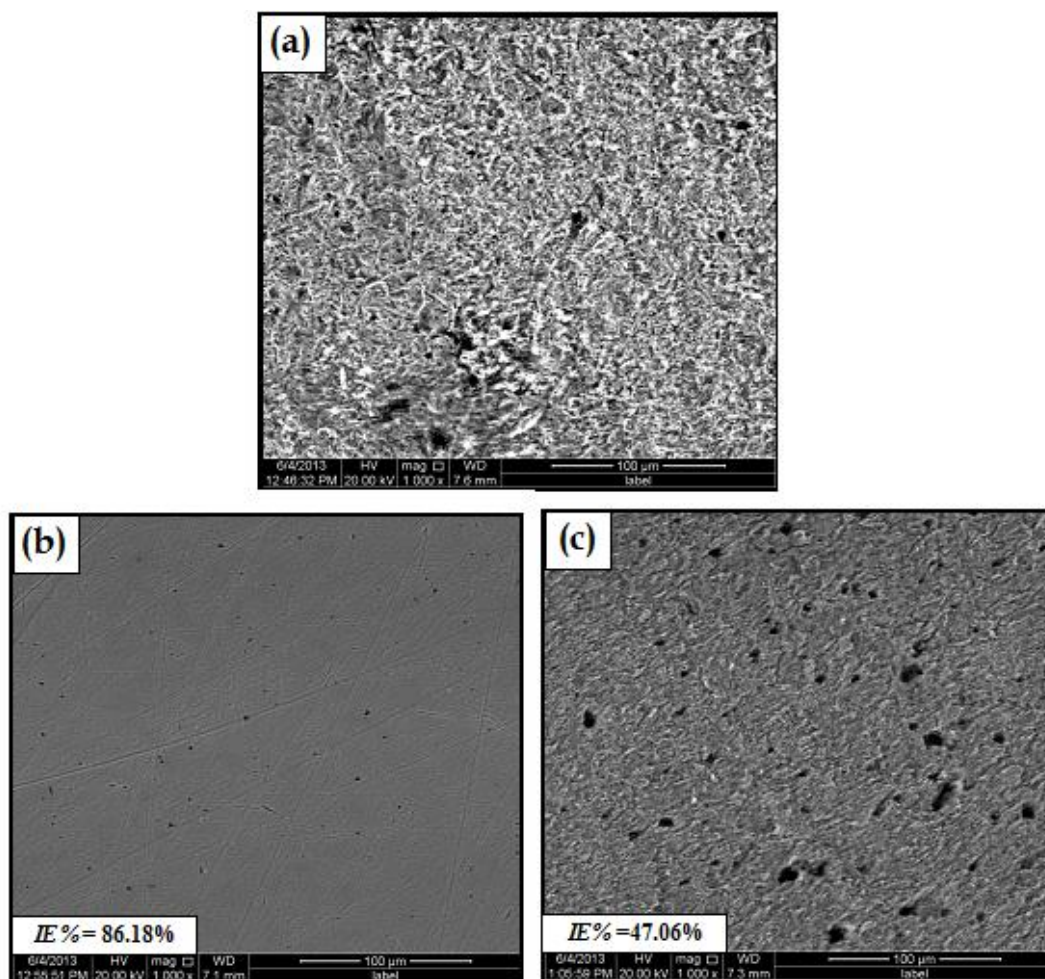


**Figure 5.** SEM for steel surface in 0.75 M  $H_3PO_4$  (a) without inhibitor, (b) with 5 mL% of ROSE and (c) with 5 mL% ROPE.

### 3.2. Adsorption isotherm

Fundamentally, for solid–liquid adsorption system, adsorption isotherm is important to explain how adsorbate interacts with adsorbents. The variation of the surface coverage ( $\theta = IE\%/100$ ) with

the concentration of extract ( $C_{Extract}$ ) can be tested by various adsorption isotherm models. It is imperative for understanding the adsorption behavior to distinguish the most proper adsorption isotherm model.

Figure 6 indicates that the adsorption data fit well the Langmuir adsorption isotherm model [16]:

$$C_{Extract} / \theta = \frac{1}{K_{ads.}} + C_{Extract} \tag{4}$$

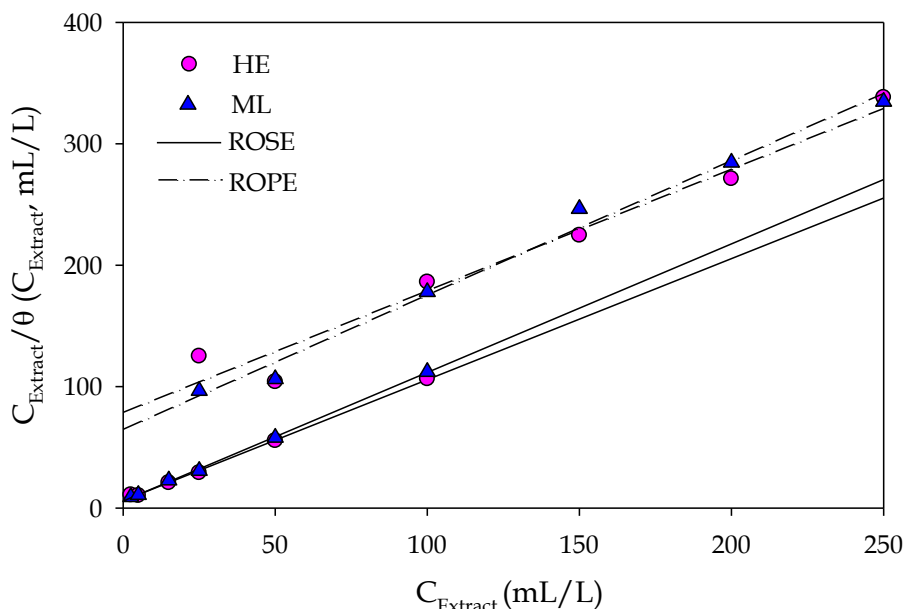


**Figure 6.** Langmuir adsorption isotherm of ROSE and ROPE on steel from 0.75 M  $H_3PO_4$ .

where  $K_{ads.}$  is the equilibrium constant of adsorption.  $K_{ads.}$  values are calculated from the intercept of the plot for adsorption process and related to the standard free energy of adsorption by the following equation [24]:

$$K_{ads.} = \frac{1}{C_{water}} \exp\left(-\frac{\Delta G_{ads.}^o}{RT}\right) \tag{5}$$

where  $C_{water}$  is the concentration of water molecules (has similar unit of  $C_{Extract}$ ),  $R$  is the universal gas constant and  $T$  is the absolute temperature. The linear regression between  $C_{Extract} / \theta$  and  $C_{Extract}$ , Langmuir parameters and standard free energy of adsorption are estimated and listed in Table 2.

The isotherm was found to be linear over the entire concentration range of both extracts and the correlation coefficients ( $r^2$ ) and slope values were approximately equal to unity, confirming that the adsorption of ROSE and ROPE on the steel surface obeys the Langmuir adsorption isotherm by forming adsorption layer of one molecule thickness. The Langmuir model refers to monolayer adsorption onto surfaces containing a set number of identical sites [33]. Inspection the values of  $K_{ads.}$ , it was found that ROSE has higher affinity to adsorb on steel surface than ROPE. It was reported that

the higher values of  $K_{ads}$ , the stronger and more compact adsorbed layer is formed which results in the higher surface coverage (i.e.  $IE\%$ ) [12].  $\Delta G_{ads}^o$  values are negative, indicating favorable adsorption of extracts species on steel surface and feasibility and spontaneous nature of adsorption with high preference of ROSE on steel surface as compared to ROPE. Once again the data in Table 2 give good consistency between HE and ML measurements.

**Table 2.** Langmuir's adsorption parameters for ROSE and ROPE on steel surface from 0.75 M  $H_3PO_4$

The extract	The Langmuir's adsorption parameters					
	The slope		$K_{ads}$ (L.mL <sup>-1</sup> )		$-\Delta G_{ads}$ (kJ. mol <sup>-1</sup> )	
	HE	ML	HE	ML	HE	ML
ROSE	1.01	1.06	0.20	0.18	13.34	13.08
ROPE	1.11	1.13	0.02	0.02	7.54	7.54

### 3.3. Effect of temperature

Temperature is an important factor governing the rate of corrosion in acid solutions without and with inhibitors. The increase of corrosion rate can be described by Arrhenius equation and may be used to predict the manners of inhibitor adsorption on metal surface.

**Table 3.** Steel corrosion rates in 0.75 M  $H_3PO_4$  without and with certain concentration of ROSE and ROPE at different temperatures

Temperature (K)	0.75 M $H_3PO_4$	0.75 M $H_3PO_4$ + 1.50 mL% ROSE	0.75 M $H_3PO_4$ + 20.00 mL% ROPE
	$\rho_{ML} \times 10^{-5}$ (g.cm <sup>-2</sup> .min <sup>-2</sup> )	$\rho_{ML} \times 10^{-5}$ (g.cm <sup>-2</sup> .min <sup>-2</sup> )	$\rho_{ML} \times 10^{-5}$ (g.cm <sup>-2</sup> .min <sup>-2</sup> )
303	3.40	1.14	1.01
313	7.82	1.20	1.86
323	15.51	2.76	4.05
333	27.43	8.03	11.40

Table 3 represents the values of steel corrosion rate ( $\rho_{ML}$ ) in 0.75 M  $H_3PO_4$  without and with certain concentration of ROSE (1.50 mL%) and ROPE (20.00 mL%) at different temperatures ranging from 303 K to 333 K. In order to give fair study for the variation of inhibition efficiency with temperature, the concentration of each extract was selected on the basis of comparable inhibition efficiencies at 303 K, see Table 1. Analysis of data in Table 3 revealed strong positive correlation between steel corrosion rate and solution temperature without and with inhibitor. Figure 7-a illustrates that the corrosion rate increases exponentially as a function of temperature increase. This result suggests that steel corrosion rate may be controlled by the metal oxidation process and that it may

follow Arrhenius law [35]. Furthermore, the *IE*% values of both extracts are influenced with increasing temperature as illustrated in Fig. 7-b.

It can be seen that the *IE*% values increase with increasing the solution temperature from 303 to 313 K, then decrease with increasing temperature up to 333 K. Raising solution temperature may influence the acid-metal reactions in a complex manner, since many changes may occur on the metal surface such as rapid etching, desorption and/or decomposition of inhibitor and increase in the solubility of inhibitor that may enhance adsorption process [36, 37].

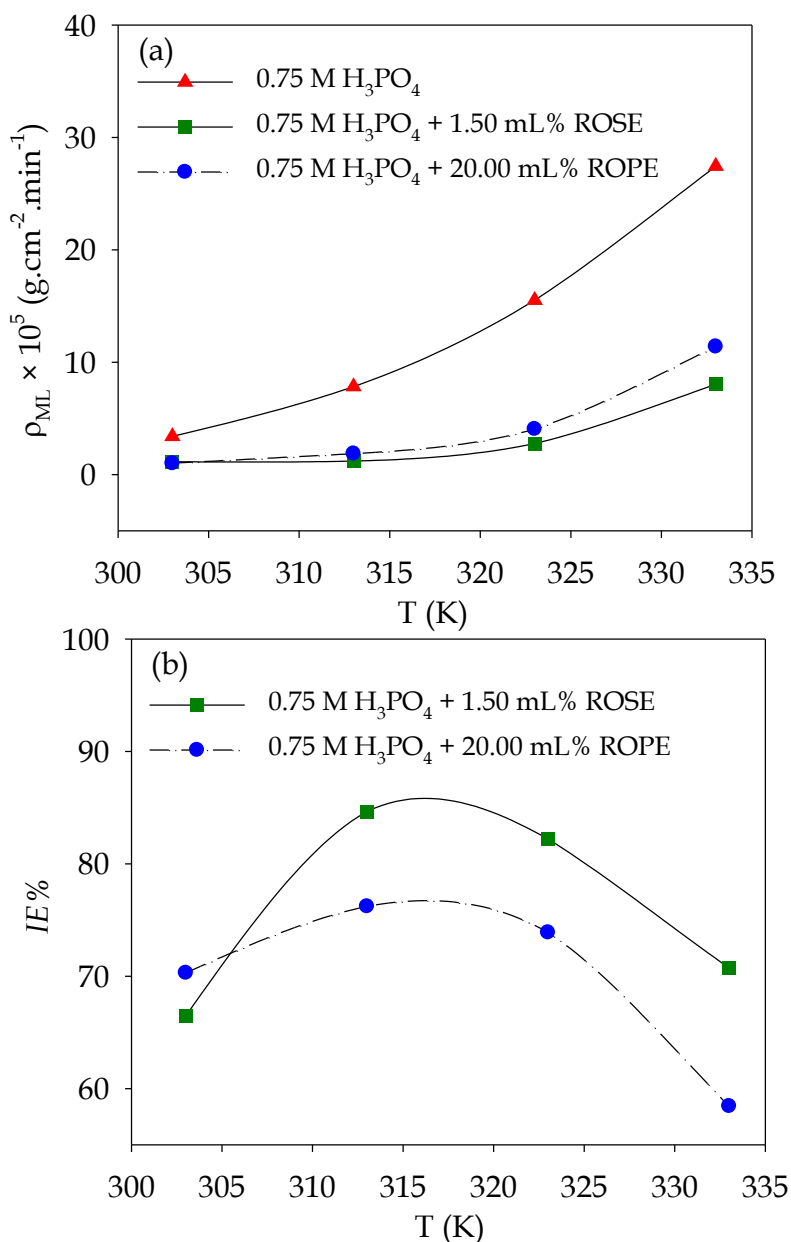


**Figure 7.** Variation of (a)  $\rho_{ML}$  and (b) *IE*% with solution temperature for steel in 0.75 M H<sub>3</sub>PO<sub>4</sub> without and with certain concentration of ROSE and ROPE at different temperatures.

Apparent activation energy ( $E_a$ ) of corrosion process is calculated using the linearized form of Arrhenius equation as follows [36]:

$$\ln \rho_{ML} = \ln A - \frac{E_a}{RT} \tag{6}$$

where  $A$  is the frequency factor. Fig. 8 shows plots of  $\ln \rho_{ML}$  against  $T^{-1}$  for steel corrosion in 0.75 M  $H_3PO_4$  without and with certain concentration of ROSE and ROPE. A straight lines are obtained with a slope of  $-\frac{E_a}{R}$  and an intercept of  $\ln A$  from which the values of  $E_a$  and  $A$  are estimated, respectively (Table 4).

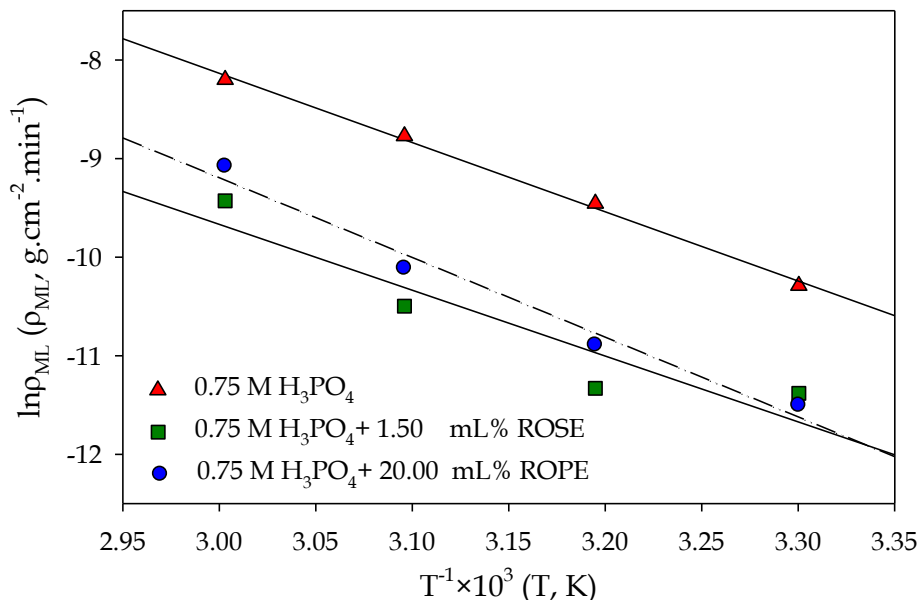


**Figure 8.** Arrhenius plots for steel corrosion in 0.75 M  $H_3PO_4$  without and with certain concentration of ROSE and ROPE at different temperatures.

**Table 4.** Arrhenius parameters for steel corrosion in 0.75 M  $H_3PO_4$  without and with 1.5 mL% ROSE and 20.0 mL% ROPE

The studied solution	$A \times 10^{-5}$ (g.cm <sup>-2</sup> .min <sup>-1</sup> )	$E_a$ (kJ. mol <sup>-1</sup> )
0.75 M $H_3PO_4$	4.14	58.39
0.75 M $H_3PO_4$ + 1.5 mL% ROSAE	0.32	55.55
0.75 M $H_3PO_4$ + 20.0 mL% ROPAE	35.20	67.26

It was found that the addition of 1.50 mL% of ROSE decreases somewhat the value of  $E_a$  as compared to that without extract. Earlier study of Riggs and Hurd [38] reported that at higher levels of inhibition the net corrosion reaction shifts from that on the uncovered part of the metal surface to the covered one, so low values of  $E_a$  was recorded. Others related this behavior to chemisorptions

mechanism [39-41]. While the addition of 20.00 mL% of ROPE increases the value of  $E_a$  as compared to that without extract, indicating that the inhibitor retards the metal dissolution by increasing the energy barrier of the corrosion reaction. Several studies on acid corrosion inhibition explained this result by the occurrence of physical adsorption (i.e. electrostatic adsorption) for the inhibitor species on the metal surface [22, 27, 42]. Equally, the frequency factor ( $A$ ) has the same trend that obtained for apparent activation energy [41].

### 3.4. Active constituents of ROSE and ROPE and inhibition mechanism

Onion (*Allium cepa*) is a resourceful vegetable that is consumed fresh as well as in the form of processed products [43]. Red onion is one of the most important sources of different biologically active phytochemicals e.g. phenolic acids, flavonoids, cepaenes, thiosulfinates and anthocyanins [44]. Chemical analysis of red onion seeds showed high concentrations of various S-cysteine derivatives [45].

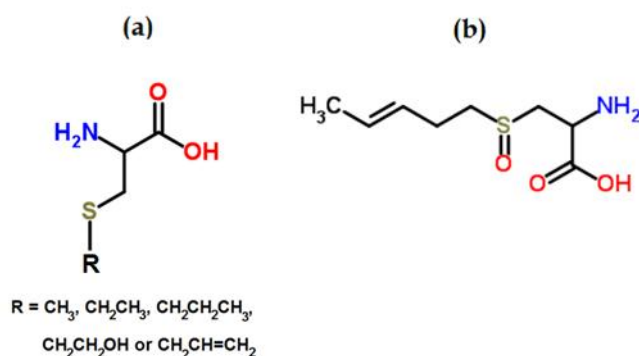


**Figure 9.** Effective constituents of ROSE: (a) S-Cysteine derivatives and (b) S-Alkenyl Cysteine Sulfoxide.

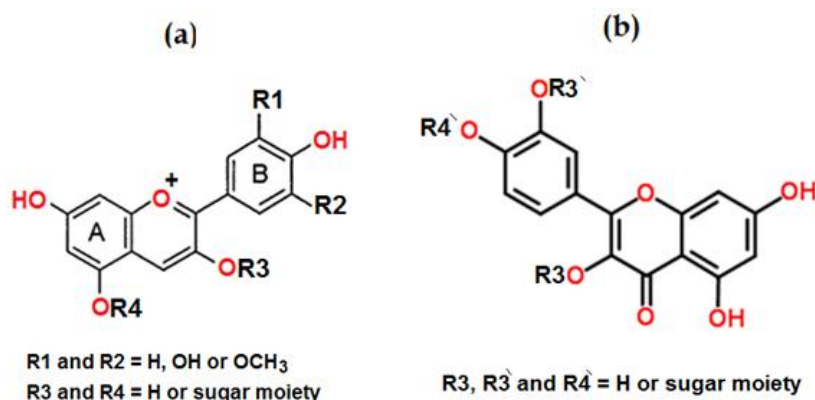


**Figure 10.** Effective constituents of ROPE: (a) Anthocyanin derivatives and (b) Quercetin derivatives.

Moreover, S-Alkenyl Cysteine Sulfoxide was identified from the red onion seeds and its antioxidant activity was evaluated [46]. While anthocyanin and quercetin derivatives are frequently found concentrated in the peel (skin) of most onions where they impart respectively the red and yellow/brown color [47-50]. So, the major effective constituents of ROSE and ROPE can be summarized in Figs. 9 and 10, respectively. Obviously Fig. 9 illustrates that cysteine derivatives possess three active centers. These are  $-SR$ ,  $-NH_2$  and  $-COOH$ . Depending on the pH value, it is well known that cysteine can be found in three forms: (i) neutral ( $-NH_2$  and  $-COOH$ ), (ii) zwitterionic ( $-NH_3^+$  and  $-COO^-$ ) and (iii) anionic ( $-COO^-$ ) [51]. Since the aggressive solution under study is relatively high acidic, the impact of both zwitterionic and anionic form is ruled out and the cationic form ( $-NH_3^+$ ) is the predominant [52]. Under such conditions,  $-NH_3^+$  and the lone pair of electrons on S atom play an important role for cysteine adsorption on steel surface. Figure 11 illustrates the proposed mechanism for the active constituent of ROSE on steel surface from 0.75 M  $H_3PO_4$  solutions.

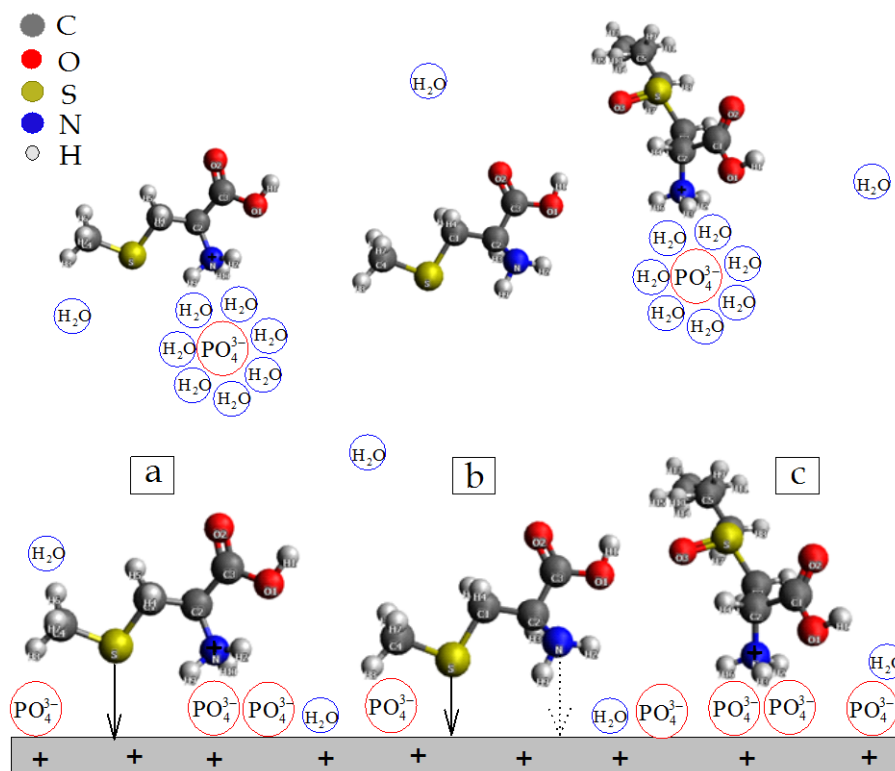


**Figure 11.** The suggested adsorption mechanism for ROSE effective constituents on steel surface from 0.75 M  $H_3PO_4$ .

For simplification the S-methyl cysteine (Figs. 11 a and b) and S-Alkenyl cysteine sulfoxide (Fig. 11 c) were used as models for simulating the adsorption process. Since steel surface is positively charged in acid solutions [53, 54], it was expected that the acid anion (i.e. phosphate ion) adsorbed electrostatically and distributed randomly on the steel surface giving rise to net negative charge.

Hence, the cysteins may adsorb electrostatically (physically) on the phosphate negative layer via  $-\text{NH}_3^+$  and it may adsorb chemically with the bare metal through the over lap of the lone pair electrons on S atom and the vacant d orbital of Fe of steel surface (Fig 11a). If the  $-\text{NH}_3^+$  group loses its proton under the positive field of the bare metal, the N atom of the resultant  $-\text{NH}_2$  group may adsorb chemically on the steel surface (Fig. 11b) but much weaker than that in the case of S atom. In Fig. 11c, the cysteine sulphoxide may adsorb electrostatically through the  $-\text{NH}_3^+$  on the phosphate layer that already adsorbed on the steel surface. In the light of these proposed models for cysteine adsorption on the steel surface under the studied conditions, one can clarify the obtained results in section 3.3. According to the suggested adsorption modes of ROSE species, increasing temperature strengthens the chemisorption process while weakens the physical one, so the inhibition efficiency decreases somewhat but still higher than that at 303 K. Corrosion inhibition study for steel in  $\text{H}_2\text{SO}_4$  using L cysteine revealed that the adsorption of cysteine on the mild steel surface has a somewhat chemisorptive character [55].

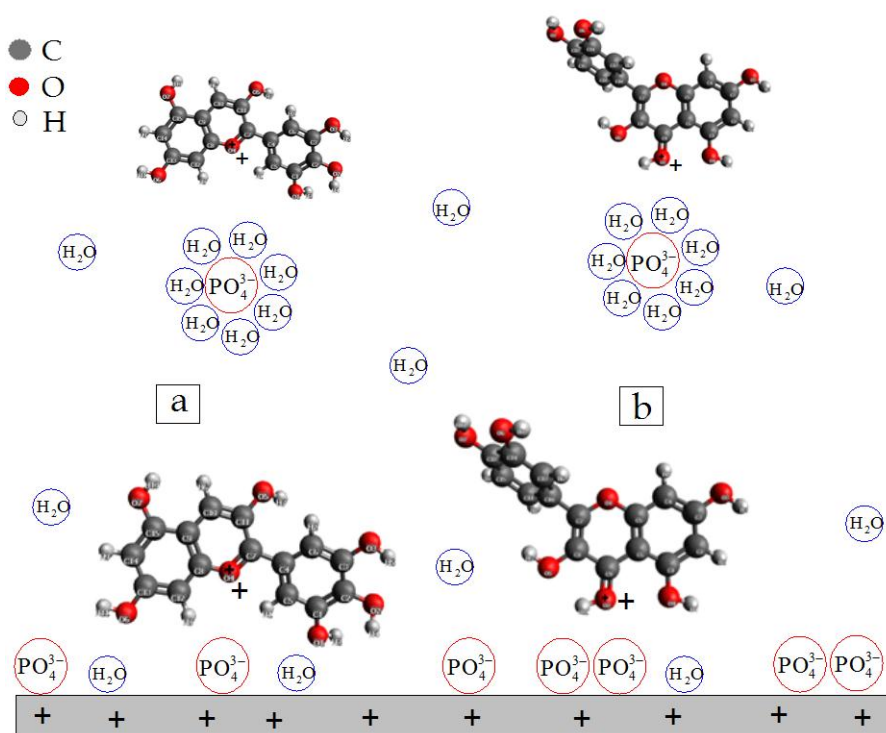


**Figure 12.** The suggested adsorption mechanism for ROPE effective constituents on steel surface from 0.75 M  $\text{H}_3\text{PO}_4$ .

Figure 12 illustrates respectively the adsorption models a and b of anthocyanin and quercetin (the major constituents of ROPE) on steel surface from 0.75 M  $\text{H}_3\text{PO}_4$  solution. For simplification the R substituent (Fig. 10) is assumed to be H in all cases. Anthocyanin is already in the cationic form while quercetin is converted to the cationic form by protonation ( $=\text{OH}^+$ ) as a result of acidic medium

[56]. It was suggested that the positively charged species of anthocyanin (Fig. 12 a) and quercetin (Fig. 12 b) would be adsorbed cooperatively and electrostatically on the negatively charged layer of phosphate ion that firstly adsorbed on the steel surface. This suggested model for the adsorption of ROPE species on steel surface is in good agreement with the results obtained in section 3.3, which revealed physical adsorption for ROPE.

#### 4. CONCLUSIONS

Based on the chemical measurements (HE and ML) and SEM used for testing and comparing the inhibitory action of ROSE and ROPE on the corrosion of steel in 0.75 M H<sub>3</sub>PO<sub>4</sub>, the following conclusions can be drawn:

- The investigated ROSE and ROPE act as good inhibitors for the corrosion of steel in 0.75 M H<sub>3</sub>PO<sub>4</sub> and the ROSE is more effective than the ROPE.
- The inhibition efficiency of both extracts increases with increasing concentration and gives powerful fitting to the Langmuir adsorption isotherm with the highest adsorption affinity for ROSE.
- The values of  $E_a$  without and with inhibitor revealed chemisorption and physical adsorption behavior for ROSE and ROPE, respectively, on the steel surface from 0.75 M H<sub>3</sub>PO<sub>4</sub>.
- Good consistency between results obtained from HE and ML measurements was obtained.
- The relation between the active adsorption centers of the major effective constituents of ROSE and ROPE and the inhibition mechanism was fully discussed and emphasized the results obtained from temperature effect.

#### References

1. J.E. Bringas (ed.), Handbook of Comparative World Steel standards (ASTM DS67B), ASTM International, USA (2004)
2. R.W. Revie, H.H. Uhlig, *Corrosion and Corrosion Control: An Introduction to Corrosion Science and Engineering*, 4<sup>th</sup> Edi., John Wiley & Sons, Inc., New Jersey (2007).
3. J.R. Davis, *Corrosion: Understanding the Basics*, ASM International, Materials Park Ohio (2000).
4. E.M. Sherif, A.T. Abbas, H. Halfa and A.M. El-Shamy, *Int. J. Electrochem. Sci.*, 10 (2015) 1777.
5. B.A. Abd-El-Nabey, A.M. Abdel-Gaber, G.Y. Elewady, M.M. El. Sadeek and H. Abd-El-Rhman, *Int. J. Electrochem. Sci.*, 7 (2012) 11718.
6. C.G. Dariva and A.F. Galio, *Corrosion Inhibitors – Principles, Mechanisms and Applications*, INTECH (2004).
7. S.K. Sharma, *Green Corrosion Chemistry and Engineering: Opportunities and Challenges*, Wiley-VCH Verlag & Co.KGaA, Weinheim, Germany (2012).
8. A. Crossland, R. R. Woollam, J. Vera, J. Palmer, G. John and S. Turgoose, *Corrosion 2011*, 13-17 March, Houston, Texas (2011).
9. Y. Jianguo, W. Lin, V. Otieno-Alego and D.P. Schweinsberg, *Corros. Sci.*, 37 (1995) 975.
10. E. Khamis, M.A. Ameer, N.M. AlAndis and G. Al-Senani, *Corrosion*, 56 (2000) 127.
11. L. Wang, *Corros. Sci.*, 43 (2001) 2281.
12. E.A. Noor, *Corros. Sci.*, 47 (2005) 33.

13. M. Benabdellah, A. Ousslim, B. Hammouti, A. Elidrissi, A. Aouniti, A. Dafali, K. Bekkouch and M. Benkaddour, *J. Appl. Electrochem.*, 37 (2007) 819.
14. A. Dadgarinezhad and F. Baghaei, *J. Chi. Soc.*, 54 (2009) 208.
15. L.M. Alaoui, B. Hammouti, A. Bellaouchou, A. Benbachir, A. Guenbour and S. Kertit, *Der Pharma Chemica*, 3 (2011) 353.
16. X. Li, S. Deng and H. Fu, *Corros. Sci.*, 55 (2012) 280.
17. A.S. Fouda, M. Diab, A. El-Sonbati and Sh.A. Hassan, *African Journal of Pure and Applied Chemistry*, 7 (2013) 67.
18. A. Ousslim, K. Bekkouch, A. Chetouani, E. Abbaoui, B. Hammouti, A. Aouniti, A. Elidrissi and F. Bentiss, *Res. Chem. Intermed.*, 40 (2014) 1201.
19. M. Abouchane, M. El Bakri, R. Tourir, A. Rochdi, O. Elkhatabi, M. Ebn Touhami, I. Forssal and M. Mernari, *Res. Chem. Intermed.*, 41 (2015) 1907.
20. G. Gunasekaran and L.R. Chauhan, *Electrochim. Acta*, 49 (2004) 4387.
21. M. Bendahoum, M. Benabdellah and B. Hammouti, *Pigm. Resin Technol.*, 35 (2006) 95.
22. M. Benabdellah, M. Benkaddour, B. Hammouti, M. Bendahhou and A. Aouniti, *Appl. Surf. Sci.*, 252 (2006) 6212.
23. M. Sivaraju and K. Kannan, *Asian J. Chem.*, 22 (2010) 233.
24. M.A. Ameer and A.M. Fekry, *Prog. Org. Coat.*, 71 (2011) 343.
25. M. Boudalia, A. Guenbour, A. Bellaouchou, A. Laqhaili, M. Mousaddak, A. Hakiki, B. Hammouti and E.E. Ebenso, *Int. J. Electrochem. Sci.*, 8 (2013) 7414.
26. A.S. Yaro, A.A. Khadom and R.K. Wael, *Alex. Eng. J.*, 52 (2013) 129.
27. X. Li, S. Deng, H. Fu and X. Xie, *Corros. Sci.*, 78 (2014) 29–42.
28. S.N. Victoria, R. Prasad and R. Manivannan, *Int. J. Electrochem. Sci.*, 10 (2015) 2220.
29. P. Vennila, S. Kavitha, G. Venkatesh and P. Madhu, *Der Pharma Chemica*, 7 (2015) 275.
30. E.A. Noor, *Mater. Chem. Phys.*, 131 (2011) 160–169.
31. E.A.Noor and A.H. Al-Moubaraki, *Int. J. Electrochem. Sci.*, 3 (2008) 806.
32. A.S. Fouda, M.N. Moussa, F.I. Taha and A.I. Elneanaa, *Corros. Sci.*, 26 (1986) 719.
33. L. Sala, F.S. Figueira, G.P. Cerveira, C.C. Moraes and S.J. Kalil, *Braz. J. Chem. Eng.*, 31 (2014) 1013.
34. M. Lagrenée, B. Mernari, M. Bouanis, M. Traisnel and F. Bentiss, *Corros. Sci.*, 44 (2002) 573.
35. C. Trépanier and A.R. Pelton, Effect of temperature and pH on the corrosion resistance of nitinol. Proceeding of ASM Materials & Processes for Medical Devices Conference, eds: M. Helmus and D. Medlin, ( 2005) 392.
36. E.A. Noor, *Int. J. Electrochem. Sci.*, 2 (2007) 996.
37. T. Peme, L.O. Olasunkanmi, I. Bahadur, A.S. Adekunle, M.M Kabanda and E.E. Ebenso, *Molecules*, 20 (2015) 16004.
38. O.L. Riggs Jr and R.M. Hurd, *Corrosion*, 23 (1967) 252.
39. S. Martinez and I. Stern, *J. Appl Electrochem.*, 31 (2001) 973.
40. S.S. Abd El-Rehim, M.A.M. Ibrahim and K.F. Khalid, *Mater. Chem. Phys.*, 70 (2001) 268.
41. E.A. Noor, A.A. Al-Ghamdi and A.H. Al-Moubaraki, *Amer. J. Appl. Sci.*, 8 (2011) 1353.
42. A. Popova, E. Sokolova, S. Raicheva and M. Christov, *Corros. Sci.*, 45 (2003) 33.
43. B.N. Singh, B.R. Singh, R.L. Singh, D. Prakash, D.P. Singh, B.K. Sarma, G. Upadhyay and H.B. Singh, *Food Chem. Toxicol.*, 47 (2009) 1161.
44. I.L. Goldman, M. Kopelberg, J.E. Devaene and B.S. Schwartz, *Throm. Haemo.*, 76 (1996) 450.
45. I. Dini, G.C. Tenore and A. Dini, *Food Chem.*, 107 (2008) 613.
46. I. Dini, G.C. Tenore and A. Dini, *J. Nat. Prod.*, 71 (2008) 2036.
47. V. Benítez, E. Mollá, M.A. Martín-Cabrejas, Y. Aguilera, F.J. López-Andréu, K. Cools, L.A. Terry and R.M. Esteban, *Plant Foods Hum. Nutr.*, 66 (2011) 48.
48. S.M. Shim., H.L. Yi and Y.S. Kim, *Int. J. Food Sci. Nutr.*, 62 (2011) 835.
49. B. Soon-Ei, *Journal of Fashion Business*, 13 (2009) 109.

50. A.S. Rodrigues, M.R. Pérez-Gregorio, M.S. García-Falcón, J. Simal-Gándara and D.P.F. Almeida, *Food Chem.*, 124 (2011) 303.
51. S. Fischer, A.C. Papageorgiou, M. Marschall, J. Reichert, K. Diller, F. Klappenberger, F. Allegretti, A. Nefedov, C. Wöll and J.V. Barth, *J. Phys. Chem. C*, 116 (2012) 20356.
52. F.A. Bettelheim, W.H. Brown, M/K. Campbell, S.O. Farrell and O.J. Torres, *Introduction to Organic and Biochemistry*, Brooks/Col, Belmont, USA, (2013) p. 330.
53. M. Lebrini, M. Lagrenee, H. Vezin, L. Gengembre and F. Bentiss, *Corros. Sci.*, 47 (2005) 485.
54. E.A. Noor and A.H. Al-Moubaraki, *Mater. Chem. Phys.*, 110 (2008) 145.
55. M. Ozcan, F. Karadağ and I. Dehri, *Acta Phys. -Chim. Sin.*, 24 (2008) 1387.
56. A.N. Chebotarev and D.V. Snigur, *J. Analyt. Chem.*, 70 (2015) 55.

© 2016 The Authors. Published by ESG ([www.electrochemsci.org](http://www.electrochemsci.org)). This article is an open access article distributed under the terms and conditions of the Creative Commons Attribution license (<http://creativecommons.org/licenses/by/4.0/>).